Electrooxidation of CO and H_2/CO Mixtures on Pt(111) in Acid Solutions

N. M. Marković,*,† B. N. Grgur,† C. A. Lucas,‡ and P. N. Ross†

Materials Sciences Division, Lawrence Berkeley National Laboratory, University of California, Berkeley, California 94720, Oliver Lodge Laboratory, Department of Physics, University of Liverpool, Liverpool, L69 7ZE, U.K.

Received: July 26, 1998; In Final Form: October 12, 1998

Electrocatalysis of CO oxidation and the interfacial structure of the CO adlayer (CO_{ad}) on the Pt(111) surface in 0.5 M H_2SO_4 were examined by using the rotating disk electrode method in combination with in situ surface X-ray diffraction measurements. The results presented here elucidate the roles played by two different forms of CO_{ad}: one which is oxidized at lower overpotentials, in the so-called preoxidation region, we characterize as a weakly adsorbed state ($CO_{ad.w}$), and a strongly adsorbed state ($CO_{ad,s}$) which is oxidized at higher overpotentials. The $CO_{ad,w}$ state forms at saturation coverage by adsorption at $E < 0.15$ V and assumes a compressed p(2×2) structure containing 3 CO molecules in the unit cell (0.75 CO/Pt). We propose that oxidative removal of $CO_{ad,w}$ is accompanied by simultaneous relaxation of the CO adlayer, and that the remaining CO_{ad} ($\approx$0.6 CO/Pt) assumes a new bonding state which we identify as $CO_{ad,s}$. The $CO_{ad,s}$ state is present in a structure lacking long-range order. Despite the reduced coverage by CO_{ad}, H_2 electrooxidation is still completely poisoned at potentials below 0.6 V. The electrooxidation of CO in solution is proposed to occur via the $CO_{ad,w}$ state at 0.6−0.8 V, and via the $CO_{ad,s}$ at higher potentials.

1. Introduction

Electrocatalysis of CO on platinum single crystals[1−17] and well-characterized bimetallic surfaces[18−22] is an area receiving substantial attention in view of its fundamental and practical importance. From the practical viewpoint, understanding the surface electrochemistry of CO on well-defined electrodes could result in the design of a new catalyst for fuel cells running on either industrial hydrogen or hydrogen feed stream derived from the reformation of methanol. From the fundamental viewpoint, the electrooxidation of CO on Pt(*hkl*), may lead to deeper insight into the relation between the electrocatalysis of CO and the surface atomic properties of the low-index Pt(*hkl*) surfaces. The electrooxidation of CO on the Pt(111) surface has been of particular interest, and it is now generally agreed, that when CO is adsorbed onto a Pt(111) electrode (denoted hereafter as CO_{ad}) in acid media under steady-state conditions and at potentials close to the hydrogen reversible potential, two CO_{ad} stripping peaks are observed in the stripping voltammetry.[23−28] In contrast, CO adsorption within the "double layer region" is exclusively associated with the formation of a single voltammetric peak. Although the spectroscopic nature of the adsorbed CO is dependent on the potential at which CO is adsorbed onto the Pt(111) surface[7,14] it has been suggested that the multiplicity of the CO electrooxidation peaks, observed in the stripping voltammetry of CO, should not be assigned individually to the oxidation of different CO_{ad} species.[15] Therefore, the relation of the particular binding geometry of CO_{ad} to the anodic features observed in the stripping voltammetry of CO_{ad} still remains unknown. Independent from efforts to determine the nature of the CO_{ad} states, previous studies of CO electrooxidation on Pt(111) do not provide answers to many important questions concerning the mechanism of the reaction.

In this work, we present measurements on the electrooxidation of CO and H_2/CO mixtures on the Pt(111) electrode mounted in a RDE configuration. We show the stripping voltammetry of CO which is preadsorbed at different potentials, attempting to develop a more detailed understanding of the effects of the CO adsorption potential on the development of the preoxidation wave in the stripping voltammetry of CO on the (111) electrode. To get insight into the nature of the preoxidation wave and to establish the dynamics of formation of "holes" in the CO adlayer, we also present experimental data for the electrooxidation of molecular hydrogen (HOR) on the Pt(111) surface which is fully or partially covered by preadsorbed CO. These experiments exploit the fact that holes, i.e., unoccupied Pt sites, within the CO adlayer will be "magnified" by the HOR, and the rate of the HOR will be quantitatively correlated with the geometry and/or concentration of holes. These results are then compared with the electrooxidation of CO from CO-saturated solution, highlighting differences in the kinetics of CO_{ad} electrooxidation with and without the process of readsorption of CO. We also reported results for the electooxidation of H_2/2% CO mixture under well-defined mass transfer conditions, which highlight differences in kinetics of the HOR with and without the process of readsorption of CO. The electrochemical measurements are augmented by recent in situ surface X-ray scattering results, which provided an independent (nonelectrochemical) measure of the structure and coverage of CO_{ad} on Pt(111) under dynamic conditions.

2. Experimental Section

Most of the experimental details were described previously.[18,21,29] Following the flame annealing-hydrogen (or argon) cooling method, the Pt(111) electrode was transferred into the disk configuration of the rotating ring disk electrode, RRDE.

* Author to whom correspondence should be addressed at Lawrence Berkeley National Laboratory, Mail Stop 2-100, Berkeley, CA 94720. Telephone: (510) 486-2956. Fax: (510) 486-5530.

† University of California.

‡ University of Liverpool.

10.1021/jp983177c CCC: $18.00
Published on Web 01/05/1999

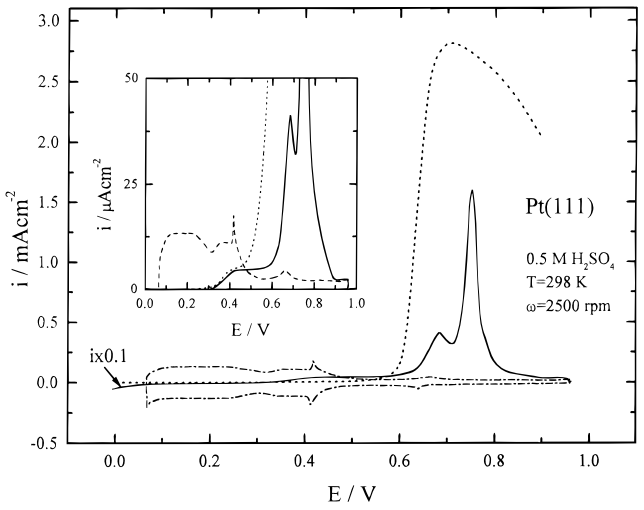

Figure 1. (—) CO stripping voltammetry on the Pt(111) surface in argon-purged solution. CO was adsorbed at the negative potential limit (0.0 V): (---) polarization curve for the HOR at the surface covered with the preadsorbed CO at 0.0 V, (— — —) the first negative sweep after stripping of CO_{ad}. Magnification of the preoxidation region for the positive-going sweep. Sweep rate was 20 mV/s.

The cleanliness of the transfer and the electrolyte, even under sustained rotation at high rotation rates, were demonstrated in our previous work.[29] For CO stripping voltammetry, the electrolyte (0.5 M H_2SO_4, Baker *Ultrex*) was saturated with CO, and the electrode was immersed into the electrolyte under potential control at five different potentials. Subsequently, the electrode was rotated at 2500 rpm for 5 min, to allow for the complete poisoning of the electrode surface with CO, before potentiodynamic data were recorded. After recording CO stripping voltammetry, the Pt(111) surface was again poisoned by CO at 0.05 V for 10 min, and then the CO was purged from solution with pure H_2. Hydrogen oxidation currents were then recorded potentiodynamically on the Pt(111) surface covered by the CO adlayer. For the electrooxidation of a dissolved pure CO gas (denoted hereafter as CO_b) and H_2 (Ar)/CO mixture the electrolyte was equilibrated for 5 min with the respective gas/mixture, while the electrode potential was held at 0.05 V, before potentiodynamic measurements were performed.

In surface X-ray diffraction measurements the X-ray cell was mounted at the center of a four-circle goniometer on beamline 7-2 at the Stanford Synchrotron Radiation Laboratory, or on 2 × 2 circle diffractometer on beamline ID 10 B at the European Synchrotron Radiation Facility, Grenoble. The outer shell of the electrochemical X-ray cell was purged with either nitrogen or CO. The CO diffused through the thin polypropylene film trapping the electrolyte, and adsorbs (dynamically) onto the Pt-(111) surface while under potential control. For more experimental details see ref 30.

The pure gases as well as the CO/Ar and CO/H_2 mixtures were purchased from Matheson (Matheson purity: 4N CO, 5N Ar, and 6N H_2). All potentials are referred to the reversible hydrogen electrode (RHE) at room temperature, and current densities are based on the geometric surface area (0.283 cm^2).

3. Results

3.1 Stripping Voltammetry of CO_{ad} and HOR on a Pt-(111)−CO_{ad} Adlayer. Figure 1 shows the base voltammogram of Pt(111) in 0.5 M H_2SO_4, onto which are superimposed the linear sweep voltammetry curves of Pt(111) covered by adsorbed CO in either argon-purged solution, i.e., anodic stripping voltammetry, or in H_2 saturated solution. The interpretation of the base voltammetry of Pt(111) in sulfuric acid has been extensively discussed in the literature.[8,11,29] Briefly summarizing, the potential region of underpotentially deposited hydrogen (denoted as H_{upd}), $\approx 0.075 < E < 0.3$ V, is clearly separated from the potential region for adsorption/desorption of bisulfate anions, $\approx 0.3 < E < 0.5$ V. The maximum charge associated with the adsorption of H_{upd} is $Q_{Hupd} \approx 160$ μC/cm^2, indicating that within the hydrogen adsorption region the Pt(111) surface is covered by ≈0.6 ML (for any adsorbate, 1 ML is defined as one molecule adsorbed per Pt surface atoms, or 1.5×10^{15} molecules/cm^2 of electrode area) of H_{upd}. Note that the theoretical charge for a full monolayer of H_{upd}, assuming one hydrogen atom for each surface platinum atom, would be 240 μC/cm^2. The charge corresponding to bisulfate adsorption is ≈80 μC/cm^2, or ≈0.3 ML, nearly equivalent to a close-packed adlayer of fully discharged HSO_4^- anions based on the crystal ionic radius. At more positive potentials, a small peak (≈15 μC/cm^2) is recorded at ca. 0.65 V. The position of this coincides with that for the so-called "butterfly" peak observed in perchloric acid solution.[31] Given that the "butterfly" peak produced in 0.1 M $HClO_4$ appears to correspond to a reversible adsorption of hydroxyl species (denoted as OH_{ad}), we suggest that the peak at 0.65 V in 0.5 M H_2SO_4 corresponds to a filling-in by OH_{ad} (H_2O being the source of OH_{ad}) on bisulfate-free Pt sites, e.g., defects in the close-packed adlayer. Formation of a full OH_{ad} adlayer on Pt(111) is inhibited in solutions containing HSO_4^- anions due to the strong adsorption, and does not occur below 1 V. In this work, the positive potential limit was chosen so as to entirely strip the preadsorbed CO from the Pt(111) surface but to avoid irreversible disordering of the surface by place-exchange of OH_{ad} and Pt, e.g., $E < 1.1$ V in Figure 1.

For the anodic stripping voltammetry curve of adsorbed CO on Pt(111) shown in Figure 1, CO is adsorbed by holding the potential at ≈0.0 V in CO-saturated solution for 5 min followed by purging the solution with Ar. Figure 1 shows that upon sweeping the potential positively from 0.0 V the onset of CO oxidation commences at ≈0.3 V, forming what we will refer to as a preoxidation wave over the potential region of ≈0.3−0.6 V (insert of Figure 1). Above 0.6 V, the stripping voltammetry is characterized by two sharp peaks, a lesser peak at ca. 0.68 V and a major peak at ≈0.75 V. For our purposes here, CO_{ad} which is oxidized within the preoxidation region will be termed as the "weakly adsorbed" state (hereafter denoted as $CO_{ad,w}$), and CO_{ad} which is oxidized above 0.6 V will be assigned as the strongly adsorbed CO_{ad} state, i.e., $CO_{ad,s}$. Deconvolution and integration of the charge under each of these features is made in Figure 2 and summarized in Table 1. As discussed previously in the literature[8,10,11] a reliable determination of the saturation coverage of CO_{ad} on Pt(111) by coulometric analysis of anodic stripping curves is far from straightforward. Weaver and co-workers[10] pointed out that in order to extract quantitative values of the coverage of CO_{ad}, it is necessary to correct the total integrated charge by the contribution from the pseudocapacitance of other surface processes that occur as the CO is removed, such as double-layer charging, adsorption of anions in sulfuric acid solution, or adsorption of OH_{ad} in perchloric acid solution. Unfortunately, there is no consensus at present about how this should be done, which is particularly problematic at the Pt(111) surface because of the large pseudocapacitances of these processes in the potential region of interest. Our estimation of these pseudocapacitances is shown in the inset of Figure 2. We suggest that in 0.5 M H_2SO_4 solution, the oxidative removal of CO is indeed

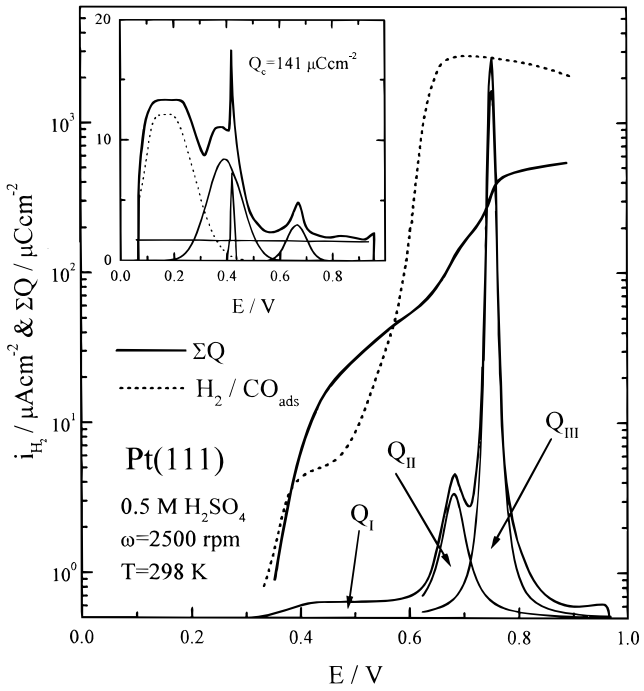

Figure 2. (—) CO stripping voltammetry (20 mV/s) of CO_{ad} on the Pt(111) surface in argon-purged solution is shown only as a reference curve: Q_I is deconvoluted charge within the preoxidation region; Q_{II} and Q_{III} are deconvoluted charges within the main stripping voltammetry: (—) the stripping charge of CO_{ad} preadsorbed at 0.0 V as a function of electrode potential, (– – –) polarization curve for the HOR on the Pt(111) covered with the CO_{ad}. Inset shows deconvolution of the charge associated with H_{upd}, $HSO_{4,ad}$, and OH_{ad} peaks.

TABLE 1: Integrated Charge and Surface Coverage (based on 480 μC cm^{-2}), for CO Stripping at Different Adsorption Potentials

	(μC cm^{-2})					
E_{ads}/V	Q_I	Q_{II}	Q_{III}	ΣQ	Q_{CO}[a]	θ
0	82	133	335	550	410	0.85
0.075	74	91	385	550	410	0.85
0.15	64	30	440	534	394	0.82
0.225			465	465	325	0.68
0.375			453	453	313	0.65

[a] $Q_{CO} = \Sigma Q - Q_{C_{dl}} - Q_{(HSO_4^-)} - Q_{OH}$.

followed by adsorption of bisulfate anions, ≈80 μC/cm^2 (charge under the peaks at 0.3−0.5 V), by adsorption of OH_{ad}, ≈15 μC/cm^2 (charge under the peak at 0.65 V) and charging of the double layer, ≈45 μC/cm^2 (charge under the constant-current line). Thus, to get a stripping charge which corresponds to the electrooxidation of CO_{ad} preadsorbed on the Pt(111) surface at ≈0.0 V, Q_{CO}, the total charge inferred from the stripping voltammetry, $\Sigma Q \approx 550$ μC/cm^2, should be corrected for the contribution of these other processes, which we estimate to be ≈410 μC/cm^2. This corresponds to a saturation coverage (θ_{CO}) of ≈0.85 ML (see Table 1). As we show below, this coverage is in reasonable agreement with the coverage determined independently from X-ray scattering, 0.75 ML. For the purposes of assigning the charge to the weakly (Q_I) and strongly (Q_{II} and $_{III}$) adsorbed states (Table 1), we assumed (somewhat arbitrarily) that these pseudocapacitances contribute only to Q_{III}, i.e., following removal of more than 50% of the CO_{ad} present.

In the HOR experiment, CO_{ad} is again adsorbed from CO solution at ≈0.0 V, followed by purging the solution with Ar, then switching to pure H_2 gas. A potentiodynamic (20 mV/s) polarization curve for the HOR on the Pt(111) surface covered

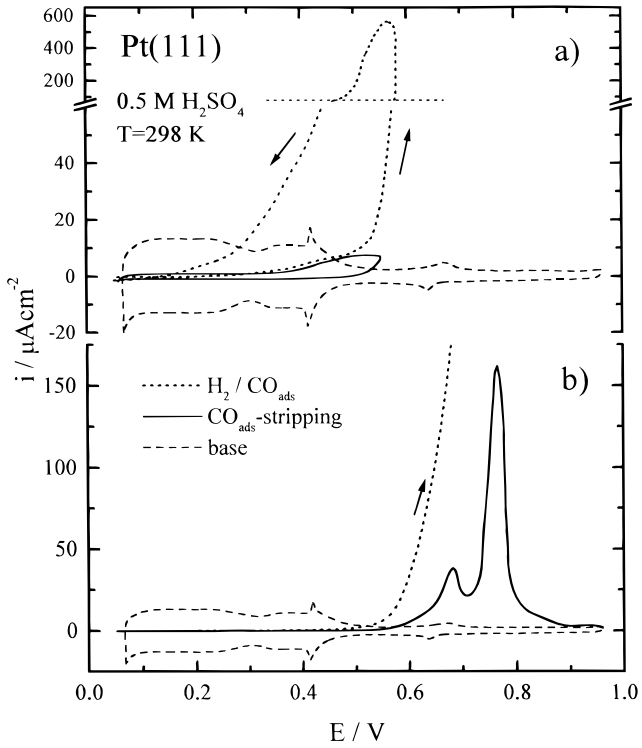

Figure 3. (a) (—) CO stripping voltammetry of the $CO_{ad,w}$ state on the Pt(111) surface in argon-purged solution; CO was adsorbed at 0.05 V and the first sweep up to 0.55 V was recorded: (– – –) polarization curve for the HOR on the Pt(111) covered with $CO_{ad,w}$: (– – –) base voltammetry for the Pt(111) surface in 0.5 M H_2SO_4. (b) After the experiment in Figure 2a, the CO stripping voltammetry (20 mV/s) of the $CO_{ad,s}$ state was recorded on the Pt(111) surface in argon-purged solution (see text for details). (– – –) polarization curve for the HOR on the Pt(111) covered with the $CO_{ad,s}$: (– – –) base voltammetry for the Pt(111) surface in 0.5 M H_2SO_4. The rotation rate was 2500 rpm. Sweep rate was 20mV/s.

with the saturation coverage of CO_{ad} was then recorded as shown in Figure 1. Starting at 0.0 V, and sweeping the potential positively, the Pt(111) surface covered with CO_{ad} exhibits no measurable current (<1 μA/cm^2) below 0.2 V, some small activity in the preoxidation potential region, then above 0.5 V the rate of the HOR increases sharply, reaching a true diffusion limiting current at 0.7 V. A diffusion limiting current is, however, observed in a very narrow potential range because oxidative removal of CO_{ad} is accompanied with concomitant adsorption of both bisulfate anions and OH_{ad}. As a consequence, the HOR current decreases continuously as the potential is swept above ≈0.75 V, just as on the CO-free Pt(111) surface; complete details of the kinetics of the HOR on the clean Pt(111) surface can be found in ref 32. It is extremely important to note the following accompanying observation: *if the potential sweep is stopped at any potential below 0.7 V, the current decays rapidly to a value approximately 10% of the instantaneous current.* Thus, the HOR current shown is only a transient current, and occurs only concurrently with the anodic stripping of the CO_{ad}.

To get further insight into the separate contributions of oxidation of the $CO_{ad,w}$ and $CO_{ad,s}$ states to the HOR kinetics, we obtained results where the anodic limit was chosen so as to strip the weakly adsorbed state of CO_{ad} but not the strongly adsorbed CO_{ad} species, i.e. ≈0.58 V. The first result is shown Figure 3a. Clearly, the HOR kinetics on the Pt(III) covered by the $CO_{ad,w}$ layer is the same as that in Figure 1, with essentially no current for H_2 oxidation until a critical amount of $CO_{ad,w}$ has been oxidized. Above 0.5 V the H_2 oxidation current

increases rapidly, increasing by about 30-fold at 0.58 V, where the potential sweep is reversed. The current then decays rapidly during the negative-going sweep, declining to essentially zero current at about 0.2 V. The current decay on the negative-going sweep is actually more a time-dependent than potential-dependent phenomenon, i.e., holding the potential at 0.58 V instead of reversing the potential sweep produced essentially the same rate of decay of the current. Thus, removal of the weakly adsorbed state, $CO_{ad,w}$, produces a transient H_2 oxidation current *only during the removal process, but the remaining $CO_{ad,s}$ adlayer relaxes and in effect re-poisons the surface for H_2 oxidation.* The second anodic sweep is shown in Figure 3b. On this sweep there is *no current* in the 0.4−0.5 V region, indicating that the relaxation of the $CO_{ad,s}$ adlayer did not re-populate the $CO_{ad,w}$ state. We found that the $CO_{ad,w}$ state can only be re-populated by repeating the exposure of the clean surface (at 0.05 V) to CO dissolved in solution. On the second anodic sweep the H_2 current appears only at the potentials where the $CO_{ad,s}$ state is oxidized, and below ca. 0.7 V only during the removal process. Steady-state H_2 oxidation currents were observed only above 0.7 V, corresponding to the removal of the more strongly bound (Q_{II}) of the $CO_{ad,s}$ states. This corresponds to the removal of about 25−30% of the total amount of CO_{ad} present from adsorption at 0.05 V.

The CO adsorption potential was found to have a dramatic effect on the creation of the $CO_{ad,w}$. A set of linear sweep voltammetry curves for the anodic stripping of CO_{ad} preadsorbed at various potentials are shown in Figure 4 along with the superimposed curves for H_2-saturated solution. Figure 4c is essentially the same curve as in Figure 1. There are three main features that characterize the effects of the CO preadsorption potential on the CO_{ad} stripping voltammetry. The first is that the preoxidation wave is observed only if CO is preadsorbed at $0.0\ V < E < 0.15\ V$. This suggests that complete removal of $CO_{ad,w}$ takes place during replacement of solution CO with purging Ar (and/or H_2) at $E > \approx 0.15$ V (the mechanism of removal is not known, but is either desorption or more likely oxidation). The second is that the major CO_{ad} stripping peak at ≈0.75 V becomes sharper and the peak maximum shifts to higher values (by ≈0.3 V) if CO_{ad} is preadsorbed at a potential more positive than $E \approx 0.0$ V. As outlined above, this change in the stripping voltammetry at $E > 0.6$ V is determined by the delicate balance between the surface coverage/nature of the CO_{ad} layer and the formation of "bare" Pt sites for adsorption of either OH_{ad} or bisulfate anions. The third characteristic is that the saturation surface coverage of CO_{ad} decreases with increasing adsorption potential, with the coverage obtained from the charge under the stripping voltammetry (corrected for the adsorption of bisulfate and charging of the double layer as indicated above) decreasing with increasing CO adsorption potential, from 410 $\mu C/cm^2$ at 0.0 V to 311 $\mu C/cm^2$ at 0.4 V (summarized in Table 1). Though many more experiments were conducted, the examples in Figure 4 demonstrate the general pattern of the CO_{ad} stripping voltammetry for CO preadsorbed at different potentials, and confirm previous findings that the number, shape, and potential of the CO stripping peaks are strongly affected by the potential at which the CO is preadsorbed onto the Pt-(111) surface.

The effects of the preadsorption potential on the transient H_2 oxidation current, i.e., the linear sweep voltammetry for the solution saturated with H_2, are shown as the dotted curves in Figure 4. These results are perhaps counter-intuitive, since they show that although the total coverage by CO_{ad} is decreasing with increasing adsorption potential, the *onset of the current for the HOR is shifted positively* as CO_{ad} is preadsorbed at more positive potentials. These results again reinforce the observation made above that below about 0.7 V these HOR currents on CO-covered surfaces are transient currents observed only *simultaneously* with CO_{ad} oxidation, i.e., if there is no CO_{ad} oxidation there is no HOR current. For preadsorption at $E > 0.15$ V, there is no preoxidation wave in the CO stripping voltammetry and no HOR current below 0.6 V, the potential for stripping the $CO_{ad,w}$ state. It was only for adsorption at 0.375 V (of examples shown), where the surface is covered by only the most strongly bonds form of CO_{ad}, that the current for the HOR becomes quasi-steady-state. As shown in the inset to Figure 4a, the magnified current shows a transient HOR current just at the "foot" of the $CO_{ad,s}$ oxidation peak, with a transition to a nontransient current above 0.7 V.

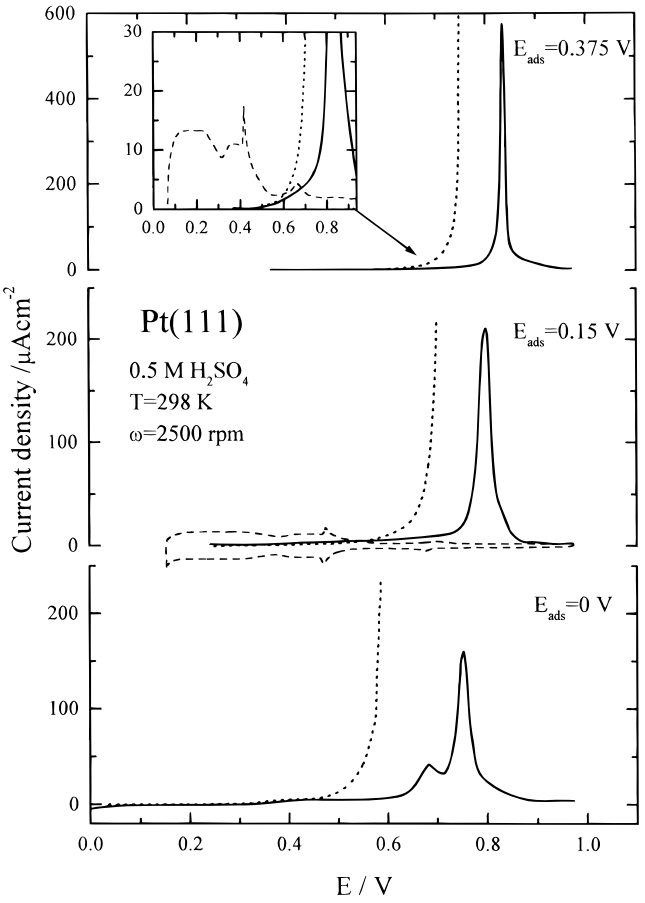

Figure 4. (—) CO stripping voltammetry of CO_{ad} which preadsorbed at different potentials on the Pt(111) surface in argon-purged solution: (— — —) polarization curves for the HOR on the Pt(111) covered with CO_{ad} preadsorbed at three different potentials. Inset shows magnification of CO_{ad} stripping voltammetry and the HOR current on the surface covered with CO_{ad} preadsorbed at 0.375 V. Sweep rate was 20 mV/s.

3.2 Electrooxidation of Bulk CO_b and H_2/CO Mixtures. For the electrooxidation of gaseous CO dissolved in the bulk electrolyte (CO_b), the electrode potential was held at 0.0 V for 5 min in order to ensure equilibration of the electrode surface with CO_{ad} prior to the measurements. The continuous supply of CO_b to the electrode surface, characteristic for the RDE, should lead to a positive shift in the onset of CO_b electrooxidation relative to onset of CO_{ad} oxidation, as was the case for CO_b oxidation on a polycrystalline platinum electrode.[18] As expected, therefore, the potential for the steep onset (i.e., the "ignition" potential) of current for CO_b electrooxidation, as shown in Figure 5, increases by ≈0.3 V compared to the

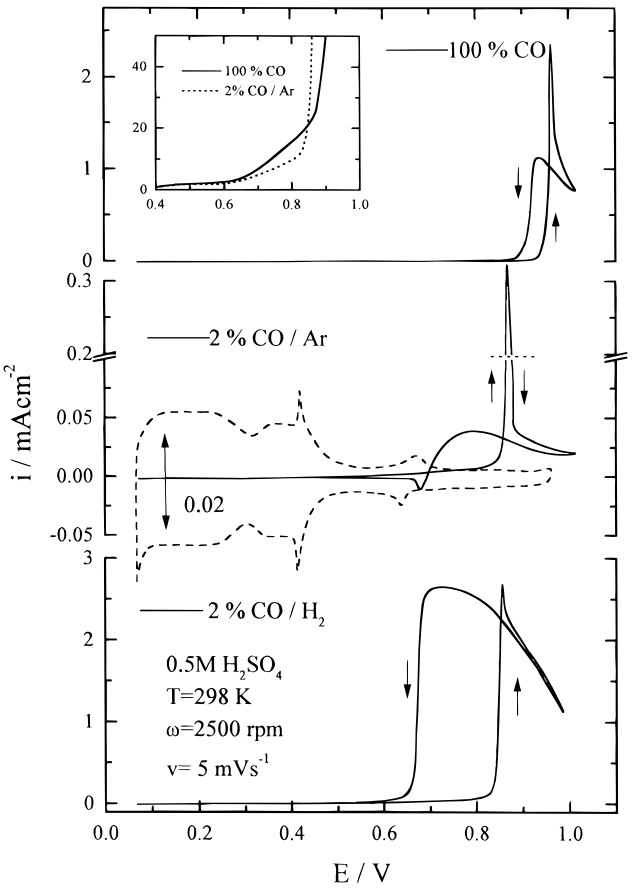

Figure 5. (a) Potentiodynamic CO oxidation current densities on Pt(111) in 0.5 M H_2SO_4 saturated with CO. Inset: Magnification of the "preoxidation region". (b) Potentiodynamic CO oxidation current for the 2% CO/Ar mixture on Pt(111). (c) Potentiodynamic HOR current densities on Pt(111) in 0.5 M H_2SO_4 saturated with 2% CO/Ar mixture. Sweep rate was 5 mV/s.

stripping peak at $E > 0.6$ V in Figure 1. Note that the diffusion-limited current plateau density is not reached below 0.95 V. The shift in the "ignition" potential relative to CO_{ad} oxidation arises from the competition between CO_b and H_2O for the free Pt sites that are created each time a CO_{ad} molecule is oxidized.[19] If the partial pressure of CO is reduced from 1 to 0.02 atm by means of a CO/Ar mixture, the "ignition" potential of CO oxidation shifts *negatively* versus pure CO (≈0.1 V in Figure 5b), producing a negative reaction order for the oxidation of CO_b on Pt at $E > 0.85$ V,[18] as observed on polycrystalline Pt. A simple Langmuir−Hinshelwood model for the competitive adsorption of CO and H_2O can account for this negative reaction order.[18,19]

The inset in Figure 5a, with a magnified current scale, indicates that oxidation of CO_b begins as early as 0.65 V, indicating that there is a preoxidation (or more accurately pre-ignition) region for the electrooxidation of CO_b. The preoxidation region was also observed in the polarization curve for the 2% CO/Ar mixture. Inspection of the potentiodynamic curves for pure CO versus 2% CO/Ar in this preignition region reveals that a reduced partial pressure of CO produced a decrease in the rate of CO_b electrooxidation, consistent with a *positive* reaction order for the CO oxidation with respect to partial pressure of CO. Recently, a positive reaction order with respect to CO_b partial pressure has also been observed within the preignition region for the electrooxidation of CO_b on polycrystalline Pt electrodes and Pt(100).[33] This implies that the reaction order with respect to CO can be either positive or negative, depending on the nature of CO_{ad} on the platinum surface. However, as was the case with H_2 oxidation currents in the preoxidation potential region, these CO_b oxidation currents in the 0.65−0.8 V preignition region are *transient currents* that occur only under potential sweeping conditions, and occur simultaneously with the oxidation of $CO_{ad,W}$. As our use of the term "ignition" implies, steady-state CO_b oxidation currents are observed only above the ignition potential, 0.85−0.9 V.

The electrooxidation of the 2% CO/H_2 mixture was measured on Pt(111) using the same potentiodynamic method used with the pure CO_b and the CO/Ar mixture. Figure 5c shows the polarization curve for oxidation of 2% CO/H_2 on Pt(111). Clearly, the transition from an inactive (i.e., poisoned) surface to a highly active unpoisoned surface occurs in a very narrow potential band, and is clearly related to the ignition of CO_b at ≈0.85 V initiates with the stripping of CO_{ad}. In fact, the steady-state currents in the 0.85−0.95 V region for 2% CO/H_2 are approximately a constant multiple of the oxidation current for 2% CO/Ar, ca. a factor of 40.

3.3 X-ray Scattering Measurements. In this section we review some recent X-ray scattering measurements which provide independent nonelectrochemical insight into the structure of the Pt(111)−CO electrochemical interface. In X-ray scattering measurements it is typical to identify changes in the surface/interfacial structure by monitoring the intensity distribution of scattering in reciprocal space, and comparing the intensity distribution with that calculated for an atomic model. A precise description of the Pt surface structure at the Pt(111)−CO electrochemical interface can be obtained by measuring both the specular and nonspecular crystal truncation rods (CTRs),[30] since H_{upd} and CO_{ad} are relatively weak scatterers making a negligible contribution to the Pt CTRs. In this case, the CTRs yield information about the position of Pt surface atoms relative to the bulk position (commonly referred to as surface relaxation) as the electrode potential is changed and the coverage by adsorbates changes. The potential dependence of the Pt(111) surface relaxation induced by the H_{upd} and/or CO_{ad} at 0.05 V is represented by the results in Figure 6. In solution free of CO, in the hydrogen adsorption potential (upd) region, the top platinum layer expands ca. ≈2% (0.05 Å) of the lattice spacing away from the second layer when H_{upd} reaches its maximum coverage.[30] Following the adsorption of CO at 0.05 V, in the same potential region (continuous flow of CO to the X-ray outer cell), the expansion is an even larger 4%. The difference in relaxation of the Pt(111) surface covered with H_{upd} and CO_{ad} probably arises from the difference in the adsorbate−metal bonding, the Pt(111)−CO_{ad} interaction being much stronger than the Pt(111)−H_{upd} interaction. After establishing the CO-induced expansion of the Pt(111) lattice, the continuous flow of CO through the outer shell of the X-ray cell was replaced with nitrogen while holding at 0.05 V. In the solution purged of CO_b, at 0.05 V we observed no change in the relaxation of the Pt surface atoms, indicating that CO_{ad} is irreversibly adsorbed on the Pt(111) surface. Upon sweeping the potential positively from 0.05 V, the oxidation of CO_{ad} in what we have referred to as the preoxidation potential region (Figure 6a) is mirrored with a small contraction of the Pt surface layer, as shown in Figure 6b. Above ca. 0.6 V, the top layer expansion is reduced significantly, contracting above 0.7 V to the same nearly unrelaxed state the Pt(111) surface has without CO_{ad}. It is important to note that the *most significant change in the surface relaxation is associated with the removal of just the weakly adsorbed state, $CO_{ad,w}$.*

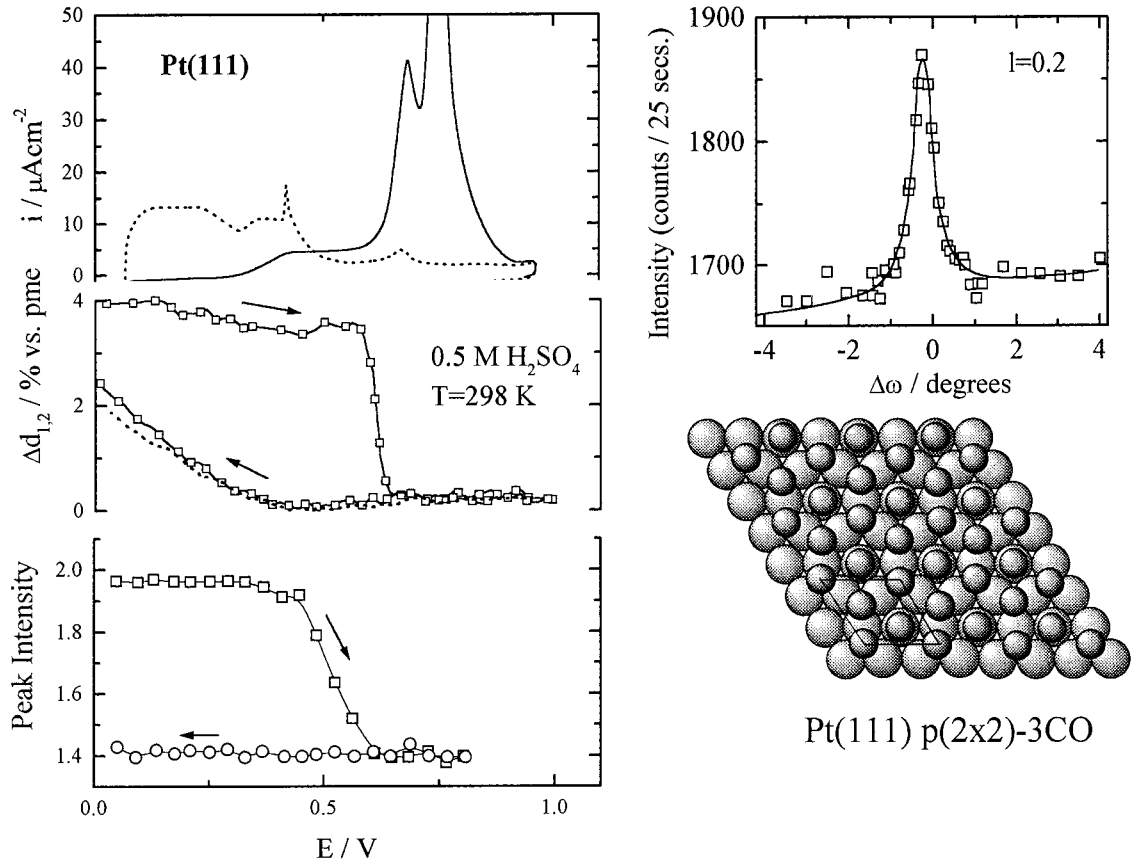

Figure 6. (a) CO stripping voltammetry on the Pt(111) surface in argon-purged solution taken from Figure 1. (b) (—) Scattering intensity changes at measured at (1, 0, 3.6) for the surface covered by CO_{ad} and (---) free of CO_{ad}; (c) Measured X-ray intensity at (1/2,1/2, 0.2) as a function of electrode potential for the same conditions as in (b). (d) A rocking scan through the (1/2,1/2, 0.2) position. (e) Ideal model for the p(2 × 2)-3CO structure. Sweep rate was 2mV/s.

Direct information regarding the CO_{ad} structure was obtained by searching in the surface plane of reciprocal space for diffraction peaks characteristic of an ordered adlayer. While holding the potential at 0.05 V and with a continuous supply of CO to the X-ray outer cell, we observed a diffraction pattern consistent with a p(2 × 2) symmetry. Once formed, the structure was stable even when the CO in the outer cell was replaced by nitrogen, confirming that CO is indeed irreversibly adsorbed on the Pt surface. Details of our analysis of the X-ray data for the adsorbed CO adlayer can be found in reference.[30] The derived structural model is shown schematically in Figure 6d, which consists of three CO molecules per p(2 × 2) unit cell. A rocking scan through the (1/2, 1/2, 0.2) position is shown in Figure 6e together with the fit of a Lorentzian line shape (solid line) to the data. From the width of this peak and from the result of similar fits to other p(2 × 2) reflections we deduced a coherent domain size for the CO adlayer in the range 80−120.[30]

Having established the presence of the p(2 × 2)-3CO adlayer at 0.05 V, following nitrogen purging of the CO, we then monitored the scattering intensity at (1/2, 1/2, 0.2) as the electrode potential was swept positively. Figure 6c shows that the potential range of stability of the p(2 × 2)-3CO phase is strongly affected by the oxidation of the weakly adsorbed state of CO_{ad}. Clearly, the close correlation of the changes in the scattering intensity and the coverage of CO_{ad} (assessed from the stripping voltammetry) suggest that the p(2 × 2)-3CO structure is present only in the potential range where the weakly adsorbed state of CO_{ad} is present on the surface. Upon the reversal of the electrode potential at ca. 0.6 V we were unable to reform the p(2 × 2)-3CO structure, confirming that this structure is governed by the formation of the weakly bonded $CO_{ad,w}$ state which is oxidized on the anodic sweep from 0.3 to 0.6 V. This supposition was tested by monitoring the scattering signal at the (1/2,1/2,0.2) position as the potential was changed, but now with a constant overpressure of CO in the X-ray outer cell. These experiments revealed a *reversible* loss and re-formation of the p(2 × 2)-3CO structure, with the p(2 × 2)-3CO structure re-forming as the potential was slowly (1 mV/s) swept below 0.2 V. This result is consistent with the electrochemical results presented above, where the $CO_{ad,w}$ state can only be re-populated by exposure of the surface to CO dissolved in solution (at E < 0.15 V).

4. Discussion

4.1 Nature of CO_{ad} and Interfacial Structure of the Pt(111)−CO_{ad} System. The results presented in this paper indicate that the key to resolving the surface electrochemistry and interfacial structures of CO on the Pt(111) surface in 0.5 M H_2SO_4 is to be found in understanding the states of CO_{ad} at the Pt(111)−liquid interface under different conditions. Several groups have demonstrated by in situ infrared reflection−adsorption spectroscopy (IRAS) that the nature of CO_{ad} on Pt(111) depends on the preadsorption potential of CO from solution. Emphasis has been placed on the examination of irreversibly adsorbed CO, i.e., in the absence of solution-phase CO, with fewer studies conducted with CO-saturated solutions. Kitamura et al.[7] found that on the Pt(111) surface three kinds of irreversibly adsorbed CO species can be observed in infrared spectra: atop, bridge, and 3-fold coordinated CO were detected within the hydrogen UPD potential region. For irreversibly

adsorbed CO on Pt(111), Leung et al.[5] found two stretching vibrations of CO molecules bonded to atop and bridge sites. In the presence of solution CO (i.e., for the highest coverages, where "compressed structures" are likely[14]) in the hydrogen UPD region the infrared spectra displayed two bands, a predominate sharp band at 2066 cm^{-1}, which is attributed to atop coordinated CO, and a weaker band centered at 1773 cm^{-1}, usually assigned to CO that is adsorbed at the 3-fold hollow sites.[14] Raising the potential to values above $E \approx 0.25$ V led to a broadening of the atop band and a replacement of the 3-fold-hollow adsorbed CO band by a feature at 1850 cm^{-1}, which is commonly assigned to bridge-bonded CO. Very recently, the Pt(111)/CO aqueous system was investigated by in situ scanning tunneling microscopy (STM) along with IRAS.[14] In these STM measurements, structures formed from both near-saturated CO solution and for irreversibly adsorbed CO were reported. In near-saturated CO solution at ≈0.05 V, the STM images showed a p(2 × 2)-3CO adlayer with a coverage of $\theta_{CO} = 0.75$ ML, exactly the same structure that we found by X-ray scattering. However, they also reported the transition to another ordered structure at $E > 0.2$ V, a $(\sqrt{19} \times \sqrt{19})$R23.4° adlayer with a coverage $\theta_{CO} = 0.68$ ML. Another CO adlayer structure, having a $(\sqrt{7} \times \sqrt{7})$R19.7° unit cell ($\theta_{CO} = 0.57$) was commonly observed for the irreversibly adsorbed CO over the potential range 0.05 to 0.45 V after the removal of solution-phase CO. A comparison of the IRAS−STM results for the irreversibly adsorbed CO and near-saturated CO solution clearly revealed that the main difference between these two systems was a higher surface coverage by CO_{ad} and the appearance of multi-coordinated CO in the latter case. This result is not surprising considering that the continuous supply of CO may lead to an increase in $\theta_{CO_{ad}}$, and thus to a different bonding geometry. It is surprising, however, that in these previous results the onset of oxidation, as well as the complete stripping of the CO ad-species, occurs at very similar potentials in both CO-free solution and CO-saturated solution.

In contrast, our results for the anodic stripping voltammetry of CO_{ad} and the electrooxidation of CO_b clearly show that the continuous supply of CO from solution to the electrode surface, whose rate can be carefully controlled by the RDE geometry, leads to a big positive shift (≈0.3 V) in the onset of CO electrooxidation, see Figures 1 and 5. Our in situ surface X-ray scattering results also showed that the only adlayer structure with long-range order was the p(2 × 2)-3CO structure. We emphasize that we also carefully searched for diffraction peaks due to $(\sqrt{19} \times \sqrt{19})$R23.4° and $(\sqrt{7} \times \sqrt{7})$R19.7° phases, but such superlattice peaks were not found at any partial pressure of CO. We conclude, therefore, that the p(2 × 2)-3CO structure is the only structure present with long-range order, and that it undergoes some form of disordering transition upon electrooxidation of relatively small amounts of the CO. We also suggest that the disordering of the p(2 × 2) structure is caused by the oxidative removal of the weakly adsorbed state of CO, implying that the ordering of the CO adlayer on the Pt(111) surface is governed by the *formation* of this weakly adsorbed state. Along the same lines, we suggest that the electrocatalytic activity of the HOR on the surface covered by an irreversibly adsorbed CO adlayer is mirrored by the initial oxidation of the weakly adsorbed state of CO_{ad}. The following discussion is based on these suppositions.

On the basis of our RDE results, and in the light of the X-ray data, we present a rationalization of the dependence of the CO stripping voltammetry on the preadsorption potential. Two potential regions can clearly be resolved in the anodic stripping voltammetry of CO_{ad}: a potential region of the electrooxidation of the $CO_{ad,w}$ state (the so-called preoxidation region) and a potential region of the electrooxidation of the $CO_{ad,s}$ state. The $CO_{ad,w}$ state is observed only if CO_{ad} is preadsorbed at potentials which are more negative of $E = 0.15$ V. Table 1 shows that the surface coverage by $CO_{ad,w}$ decreases from 82 $\mu C/cm^2$ for preadsorption at 0.05 V to zero for preadsorption at ≈0.2 V. We propose that the weakly adsorbed state of CO arises from the changes in the enthalpy of adsorption of CO on Pt(111) as a function of coverage of CO_{ad} due to strong repulsive interaction as the coverage approaches the tight packing observed in the p(2 × 2)-3CO structure. Precedence for such enthalpy changes are seen in the gas-phase data[34] for the CO/Pt(111) system, where the enthalpy of adsorption of CO decreases from 140 kJ/mol at $\theta_{CO} = 0$ ML to 45 kJ/mol at $\theta_{CO} = 0.65$ ML, with most of this decrease occurring between $0.05 < \theta_{CO} < 0.65$. If one extrapolates the gas-phase data to the higher coverages we achieve at the electrochemical interface, $\theta_{CO} = 0.75$ ML, the enthalpy falls to only 25−30 kJ/mol, which is indeed very weak chemisorption. Intuitively, one expects this weakly bound state to be the most easily oxidized, but for electrooxidation it is generally presumed that we need to nucleate an OH_{ad} species on the Pt surface,[35] and this becomes much harder to do at high coverages of CO_{ad}. If we assume that at any given potential the surface coverage by $CO_{ad,w}$ in CO-saturated solution is constant (i.e., can be re-populated from solution CO_b), then, during the replacement of CO_b with argon for the anodic stripping measurement, a change in the surface coverage of $CO_{ad,w}$ can be caused by oxidation of $CO_{ad,w}$ by OH_{ad} and/or by reversible desorption of this state from the surface. Although it is experimentally impossible (for the time being) to confirm unambiguously which process is the predominant one, we propose that observed decrease in the surface coverage of $CO_{ad,w}$ is related to an increase in the rate of the *oxidative* removal of $CO_{ad,w}$ as the preadsorption potential is increased. Therefore, the extent of $CO_{ad,w}$ is mainly governed by the amount of adsorbed oxygenated species that can be nucleated at low potential (and in the absence of CO in solution). If the preadsorbing potential is more positive of 0.25 V, the surface coverage by oxygen-containing species is high enough to entirely oxidize the $CO_{ad,w}$ while CO_b is being replaced by Ar. It is important to note, however, that oxidative removal of $CO_{ad,w}$ is always accompanied by simultaneous relaxation of the CO adlayer, and that the remaining CO_{ad} species presumably gives rise to a new bonding state, which we identify as a strongly adsorbed state, $CO_{ad,s}$. The $CO_{ad,s}$ state cannot be oxidized in this potential region because it is too strongly bound and prevents OH_{ad} nucleation.

Very little is known about the physical nature, e.g., the bonding geometry of the $CO_{ad,s}$ state or about the relaxation process following oxidation of $CO_{ad,w}$ that creates this state. We are not aware of any FTIR studies with the Pt(111) surface which creates this state in the way we have done here. It should be emphasized that at steady-state measurements the $CO_{ad,s}$ and $CO_{ad,w}$ as we have defined them here *do not coexist on the surface*. Since it is the lateral repulsion interaction between CO_{ad} molecules at high coverage (>0.5 ML) that creates the $CO_{ad,w}$ state, *all* the CO_{ad} molecules on the surface are in the weakly adsorbed state. This is the case even though the structure determined by X-ray scattering shows two in-equivalent binding sites, i.e. CO−Pt coordination, atop, and 3-fold hollow. When the coverage is reduced by oxidation, and the repulsive interaction is correspondingly reduced, the remaining CO_{ad} molecules relax into a less closely packed CO−CO coordination,

which lacks long-range order. It is this relaxed state which we characterized as $CO_{ad,s}$. The results shown in Figure 2b confirm that the $CO_{ad,s}$ state is very stable below $E \approx 0.6$ V, and that the electrooxidation of $CO_{ad,s}$ is observed only in the potential range where surface coverage by oxygen-containing species is observed in the base voltammogram, i.e., in the potential region of OH_{ad} adsorption (Figure 1). The need for a relatively high coverage by oxygenated species (in this case we suggest OH_{ad}) to oxidize $CO_{ad,s}$ suggests an appreciable activation barrier for surface diffusion of the $CO_{ad,s}$ state. Given that the mobility of the $CO_{ad,s}$ is significantly reduced versus the $CO_{ad,w}$ state, it is possible that at $E < 0.6$ V the $CO_{ad,s}$ state and oxygen-containing species may coexist on the surface (probably as separate domains) without interacting with each other. It appears, therefore, that due to both the small surface coverage by oxygen-containing species at $E < 0.6$ V, and the low mobility of $CO_{ad,s}$ the probability of interaction between these coadsorbing species is negligible, and, therefore, the rate of the reaction is very low.

4.2 Electrooxidation of CO_b and H_2/CO Mixtures. The stripping of a CO_{ad} monolayer on Pt(111) in CO-free solution is an interesting, but somewhat artificial, probe for the assessment of the true electrocatalytic activity of Pt(111) for the electrooxidation of CO_b. Quite clearly, in the case where the CO_b is supplied continuously to the electrode, the CO_{ad} surface coverage will be maintained at a high level and thus the nucleation of OH_{ad} (e.g., the CO electrooxidation kinetics) will be suppressed. For example, the onset of electrooxidation of CO from solution saturated with pure CO (Figure 5) is, in stark contrast to the stripping voltammetry (Figure 1), shifted positively by ≈0.3 V. Interestingly, the potential range of stability of the p(2 × 2)-3CO structure under similar conditions (with CO in solution but without rotation) is also shifted positively by ca. 0.25 V. This, in turn, implies that the weakly adsorbed state of CO can be continuously re-populated from CO_b over a wide potential range, even at the relatively low rate of transport by molecular diffusion in stationary electrolyte. The polarization curves recorded with CO in solution revealed, as in the case of CO_{ad} stripping voltammetry, that two potential regions can clearly be resolved; i.e., a slow rate of CO electrooxidation (the preignition region) and a high rate of CO electrooxidation (ignition). For our purposes here, we will focus on the pre-ignition region since the question remains as to the mechanism by which CO_b is oxidized in this potential region. We have discussed above that in the preoxidation potential region ($E < 0.6$ V) the reaction pathway for CO_{ad} oxidation is via a weakly bonded state created by the "crowding" of the surface with adsorbed CO_{ad} that reduces its adsorption energy via $CO_{ad}-CO_{ad}$ repulsion. Note that the electrooxidation of $CO_{ad,w}$ occurs in the potential region below which OH_{ad} is observed in the base voltammetry. The role of OH_{ad} in the reaction at higher potentials is more obvious, and it is likely that the kinetics of the CO_b reaction depends on a balance between the rate of OH_{ad} nucleation and the *turnover* of CO_{ad} on the surface. The positive reaction order in CO partial pressure in the preignition potential region indicates that this turnover is probably via the weakly adsorbed state, $CO_{ad,w}$. There appears to be a similar role for a weakly adsorbed state of CO_{ad} on the Pt(111) surface when CO is oxidized in the gas phase.[36,37] Recently, the vibrational spectrum of CO on Pt(111) was monitored over 13 orders of magnitude in CO pressure by using infrared/visible sum frequency generation SFG.[36,37] These results revealed that the gas-phase rate of CO oxidation is proportional to surface coverage by a *reversibly* adsorbed (and thus weakly bonded) state of CO that forms only at the relatively high partial pressures of 0.1−1.0 bar. In the ignition potential region, where more OH_{ad} nucleates on the surface, the much higher rate of oxidation probably depletes the $CO_{ad,w}$ state and the reaction proceeds via the $CO_{ad,s}$ state.

Finally, we comment on the transient currents measured in the so-called preoxidation potential region. In this potential region, below 0.6 V, there is no clear evidence for OH_{ad} nucleation. In linear sweep voltammetry, oxidation of CO_{ad} preadsorbed at $E < 0.15$ V is observed, but only in the absence of CO in solution, i.e., there is no *turnover* of CO_{ad} in this potential region. A further consequence of the absence of turnover of CO_{ad} in this potential region is that we could not observe a measurable (let alone practical) steady-state current for either CO_b or H_2/2% CO oxidation in this potential region. Thus, the transient currents for H_2 oxidation on a CO predosed Pt(111) surface that are measured in the so-called preoxidation region arise from the one-time concurrent oxidation of the adsorbed CO, and are not of practical consequence.

5. Summary

Electrocatalysis of CO oxidation and the interfacial structure of the CO adlayer (CO_{ad}) on the Pt(111) surface in 0.5 M H_2SO_4 were examined by using the rotating disk electrode method in combination with in situ surface X-ray diffraction measurements. The results presented here elucidate the roles played by two different forms of CO_{ad}: one which is oxidized at lower overpotentials, in the so-called preoxidation region, we characterize as a weakly adsorbed state ($CO_{ad.w}$), and a strongly adsorbed state ($CO_{ad,s}$) which is oxidized at higher overpotentials. The characterization as weakly adsorbed refers to the high coverage state in which the adsorption energy (enthalpy of adsorption) is reduced due to the repulsive $CO_{ad}-CO_{ad}$ interaction. The $CO_{ad,w}$ state forms at saturation coverage by adsorption at $E < 0.15$ V and assumes a compressed p(2 × 2) structure containing 3 CO molecules in the unit cell (0.75 CO/Pt). We propose that oxidative removal of $CO_{ad,w}$ is accompanied by simultaneous relaxation of the CO adlayer, and that the remaining CO_{ad} (≈0.6 CO/Pt) assumes a new bonding state which we identify as $CO_{ad,s}$. The $CO_{ad,s}$ state is present in a structure lacking long-range order. Despite the reduced coverage by CO_{ad}, H_2 electrooxidation is still completely poisoned at potentials below 0.6 V. The electrooxidation of CO in solution is proposed to occur via the $CO_{ad,w}$ state at 0.6−0.8 V, and via the $CO_{ad,s}$ state at higher potentials. Transient currents for H_2 oxidation on a CO predosed Pt(111) surface are measured in the so-called preoxidation region that arise from the one-time concurrent oxidation of the adsorbed CO, but these currents are not of practical consequence.

Acknowledgment. Work was carried out, in part, at the European Synchrotron Radiation Facility (ESRF), Grenoble, France. Detlef Smilgies and Nathalie Boudin are gratefully acknowledged for their support of ESRF beamline ID-10B and their contributions to the X-ray scattering experiments. This work was supported jointly by the Offices of Basic Energy Sciences, and Office of Advanced AutomotTransportation Technologies, Electric and Hybrid Propulsion Division of the U.S. Department of Energy under Contract No. DE-AC03-76SF00098.

References and Notes

(1) Beden, B.; Bilmes, S.; Lamy, C.; Leger, J. M. *J. Electroanal. Chem.* **1983**, *149*, 295.

(2) Kitamura, F.; Takeda, M.; Takahashi, M.; Ito, M. *Chem. Phys. Lett.* **1987**, *143*, 318.

(3) Beden, B.; Juanto, S.; Leget, J.; Lamy, C. J. *J. Electroanal. Chem.* **1987**, *238*, 323.
(4) Sun, S.; Clavilier, J.; Bewick, A. *J. Electroanal. Chem.* **1988**, *240*, 147.
(5) Leung, L.-W; Wieckowski, A.; Weaver, M. J. *J. Phys. Chem.* **1988**, *92*, 6985.
(6) Zurawski, D.; Wasberg, M.; Wieckowski, A. *J. Phys. Chem.* **1988**, *94*, 2076.
(7) Kitamura, F.; Takahashi, M.; Ito, M. *Surf. Science* **1989**, *223*, 497.
(8) Feliu, J. M.; Orts, J. M.; Fernandez-Vega, A.; Aldz, A.; Clavilier, J. *J. Electroanal. Chem.* **1990**, *296*, 191.
(9) Kinomoto, Y.; Watenabe, S.; Ito, M. *Surf. Science* **1991**, *242*, 538.
(10) Weaver, M. J.; Chang, S.-C.; Leung, L.-W.; Jiang, X.; Rubel, M.; Szklarczyk, M.; Zurawski, D.; Wieckowski, A. *J. Electroanal. Chem.* **1992**, *327*, 247.
(11) Clavilier, J.; Albalt, R.; Gomez, R.; Feliu, J. M.; Aldaz, A. *J. Electroanal. Chem.* **1992**, *330*, 489.
(12) Orts, J. M.; Fernandez-Vega, A.; Feliu, J. M.; Aldz, A.; Clavilier, J. *J. Electroanal. Chem.* **1992**, *327*, 191.
(13) Kita, H.; Narumi, H.; Ye, S.; Naihara, H. *J. Appl. Electrochem.* **1993**, *23*, 589.
(14) Villegas, I.; Weaver, M. J. *J. Chem. Phys.* **1994**, *101*, 1648.
(15) Kita, H.; Naohara, H.; Nakato, T.; Taguchi, S.; Aramata, A. *J. Electroanal. Chem.* **1995**, *386*, 197.
(16) Hayden, B. E.; Murray, A. J.; Parsons, R.; Pegg, D. J. *J. Electroanal. Chem.* **1996**, *409*, 51.
(17) Marković, N. M.; Grgur, B. N.; Lucas, C. A.; Ross, P. N. *Surf. Sci.* **1997**, *384*, L 805.
(18) Gasteiger, H. A.; Marković, N. M.; Ross, P. N. *J. Phys. Chem.* **1995**, *99*, 8290.
(19) Gasteiger, H. A.; Marković, N. M.; Ross, P. N. *J. Phys. Chem.* **1995**, *99*, 8945.
(20) Ianniello, R.; Schmidt, V. M.; Stimming, U.; Stumper, J.; Wallua, A. *Electrochem. Acta* **1994**, *39*, 1836.
(21) Gasteiger, H. A.; Marković, N. M.; Ross, P. N. *Catal. Lett.* **1996**, *36*, 1.
(22) (a) Grgur, B. N.; Zhuang, G.; Marković, N. M.; Ross, P. N. *J. Phys. Chem.* **1997**, *101*, 3910. (b) Grgur, B. N.; Marković, N. M.; Ross, P. N. *J. Phys. Chem.* **1998**, *102*, 2494.
(23) Kunimatsu, K.; Seki, H.; Golden, W. G.; Gordon, J. G.; Philpott, M. R. *Langmuir* **1986**, *2*, 464.
(24) Sobkowski, J.; Sobkowski, J. *J. Phys. Chem.* **1975**, *29*, 365.
(25) Kazarinov, V. E.; Andreev, V. N.; Shlepakov, A. V. *Electrochem. Acta* **1989**, *34*, 905.
(26) Beden, B.; Lamy, C.; de Tacconi, N. R.; Arvia, A. J. *Electrochem. Acta* **1990**, *35*, 691.
(27) Couto, A.; Perez, M.; Rincon, A.; Gutierrez, C. *J. Phys. Chem.* **1996**, *100*, 19538.
(28) Wieckowski, A.; Rubel, M.; Guitrrez, C. *J. Electroanal. Chem.* **1995**, *382*, 97.
(29) Marković, N. M.; Gasteiger, H. A.; Ross, P. N. *J. Phys. Chem.* **1995**, *99*, 3411.
(30) Lucas, C. A.; Marković, N. M.; Ross, P. N. *Phys. Rev. Lett.*, submitted.
(31) See, for example, H. A. Gasteiger, N. M. Marković and P. N. Ross, *Langmuir* **1996**, *12*, 1414, and refs therein.
(32) Marković, N. M.; Grgur, B. N.; Ross, P. N. *J. Phys. Chem.* **1997**, *101*, 5405.
(33) Grgur, B. N.; Marković, N. M.; Ross, P. N. Unpublished.
(34) Ertle, G.; Neuman, M.; Streit, K. *Surf. Sci.* **1977**, *64*, 393.
(35) The molecular identity of oxygen-containing species forming on Pt surface at potentials below ca. 1.2 V is uncertain. Water dissociation on Pt leading to the formation of adsorbed hydroxyl or other oxygenated species is a deceptively complicated reaction and is still only qualitatively understood despite extensive research.
(36) Su, X.; Cremer, P. S.; Chen, Y. R.; Somorjai, G. A. *Phys. Rev. Lett.* **1996**, *77*, 3858.
(37) Su, X.; Cremer, P. S.; Chen, Y. R.; Somorjai, G. A. *J. Am. Chem. Soc.* **1997**, submitted.